Proceedings of the Institute of Acoustics

LONG DISTANCE SOUND PROPAGATION OVER GROUNDS

J.N.B. Harriott (1), S.N. Chandler-Wilde (2), D.C. Hothersall (1)

(1) Dept. of Civil Engineering, University of Bradford, Bradford U.K.
(2) Dept. of Mathematics, Coventry Polytechnic, Coventry, U.K.

INTRODUCTION

The general problem of interest here is propagation from a point source in a homogeneous still atmosphere above flat locally reacting impedance ground. Efficient calculation methods for the potential field above acoustically homogeneous ground are well developed. In recent years sound propagation over impedance inhomogeneities has been theoretically examined [1,2,3,4,5,8,10]. A limitation common to all of the accurate calculation methods is their computational expense. Generally expense increases with $k\ell$, where k is the wavenumber of the sound and ℓ is a characteristic length of the problem.

Here we focus on propagation over a single straight line impedance discontinuity which lies perpendicular to the direct source-receiver propagation path. A development to an existing calculation method is described. This development allows efficient examination of long distance propagation.

The improved calculation method is applied to grazing incidence propagation from a source above a rigid surface to a distant receiver above absorbing ground. Excess attenuation results are applied to a notional broad-band environmental noise source. The limitations to bear in mind here are that a homogeneous still atmosphere and perfectly flat ground have been assumed. The impedance distribution in the ground is also strictly defined to allow a simple solution.

NUMERICAL METHOD

A point source with harmonic time dependence is situated over a flat locally reacting surface of infinite extent. The surface is divided by a straight line into two half planes. Each half plane is acoustically homogeneous and characterised by a frequency dependent complex admittance (the inverse of the normalised acoustic impedance). We are interested in evaluating the acoustic potential at a point in a vertical plane that passes through the source and is perpendicular to the admittance discontinuity. We will choose the x-axis to be along the intersection of this plane with the surface, the origin beneath the source, and the positive x-axis below the receiver.

Consider first the related problem in which the source is an infinitely long coherent line source, parallel to the admittance discontinuity. From the mathematical expression of this problem as a two dimensional boundary value problem (consisting of the Helmholtz equation and suitable boundary conditions) the following boundary integral equation can be derived [6]:

$$\Phi(\underline{t}_2,\underline{t}_1) = G_{\beta_2}(\underline{t}_1,\underline{t}_2) + ik(\beta_1-\beta_2)\int_{\gamma_1}\Phi(\underline{s},\underline{t}_1)G_{\beta_2}(\underline{s},\underline{t}_2)dx. \qquad (1)$$

Here $\Phi(\underline{t}_2,\underline{t}_1)$ is the acoustic potential at $\underline{t}_2$ due to a source at $\underline{t}_1$. G_{β_2} is the known Green's function for propagation from a point source in two dimensions over a homogeneous straight boundary of admittance β_2. $\gamma_1=(-\infty,X]$ is that half of the boundary with admittance β_1. $\underline{s}$ is a point $(x,0)$ in the boundary. k is the wavenumber.

Equation (1) can be solved numerically for $\Phi(\underline{t}_2,\underline{t}_1)$ by a two stage process [1,7(Ch.4),10]. We consider here an approximate but less computationally expensive solution method based on replacing $\Phi(\underline{s},\underline{t})$ by $G_{\beta_1}(\underline{s},\underline{t})$ in equation (1) [1,4,8]. This is a physically plausible approximation which gives sufficiently accurate results for application to outdoor sound propagation.

The acoustic potential, φ, in the original three dimensional problem is now approximated as follows:

$$\varphi \approx \frac{e^{ikd}}{kd} + Q\frac{e^{ikD}}{kD} \quad ; \qquad (2)$$

where kd and kD are the dimensionless distances from source (at $\underline{t}_1$) and image source to receiver (at $\underline{t}_2$). Q is the cylindrical wave reflection coefficient calculated from $\Phi(\underline{t}_2,\underline{t}_1)$. In the far field Q provides an acceptable approximation to the spherical wave reflection coefficient [1]. To calculate Φ we use the above mentioned approximate solution of the boundary integral equation:

$$\Phi(\underline{t}_2,\underline{t}_1) \approx G_{\beta_2}(\underline{t}_1,\underline{t}_2) + i(\beta_1-\beta_2)I_{\gamma_1} \ , \qquad (3)$$

where

$$I_{\gamma_1} = k\int_{\gamma_1} G_{\beta_1}(\underline{s},\underline{t}_1)G_{\beta_2}(\underline{s},\underline{t}_2)dx \ . \qquad (4)$$

Now we note that, for a reception point $\underline{s}$ in the reflecting surface and a source $\underline{t}$ above the surface,

$$G_\beta(\underline{s},\underline{t}) = H_0^{(1)}(k|\underline{t}-\underline{s}|)R_\beta(\underline{s},\underline{t}) \quad ;$$

where $H_0^{(1)}$ is the Hankel function of the first kind of order zero, and $R_\beta(\underline{s},\underline{t})$ is equal to one plus the complex cylindrical wave reflection coefficient for a homogeneous surface of admittance β. For $|\underline{t}-\underline{s}|$ large enough the real and imaginary parts of $H_0^{(1)}(k|\underline{t}-\underline{s}|)$ oscillate in a well defined fashion while $R_\beta(\underline{s},\underline{t})$ varies less rapidly. This observation suggests that I_{γ_1} can be usefully written in the more familiar form of a generalised Fourier integral:

$$I_{\gamma_1} = \int_{\gamma_1} f(x)e^{ikg(x)}dx \ , \qquad (5)$$

where

$$f(x) = kG_{\beta_1}(\underline{s},\underline{t}_1)G_{\beta_2}(\underline{s},\underline{t}_2)e^{-ikg(x)},$$

$$g(x) = g_1(x) + g_2(x),$$

and

$$g_1(x) = |\underline{t}_1-\underline{s}|, \quad g_2(x) = |\underline{t}_2-\underline{s}|.$$

When $\underline{s}$ is sufficiently distant from $\underline{t}_1$ and $\underline{t}_2$ $f(x)$ is a slowly varying function compared to $e^{ikg(x)}$. This fact allows us to use simple asymptotic methods to help evaluate (5).

An uncomplicated first case to consider is when γ_1 does not include the geometrical reflection point, x_r (the solution of $g'(x_r)=0$). For this case we may integrate by parts twice and apply the Riemann-Lebesgue lemma [9(p.277)] to the remaining integral to get

$$I_{\gamma_1} \sim J_1(X) + J_2(X) \;, \; k \to \infty, \tag{6}$$

where,

$$J_1(X) = \frac{f(X)\, e^{ikg(X)}}{ikg'(X)} \;,$$

$$J_2(X) = \left[\frac{g''(X)}{g'(X)} - \frac{f'(X)}{f(X)}\right] \frac{f(X)e^{ikg(X)}}{(ikg'(X))^2}$$

Expression (6) shows the first two terms of an asymptotic expansion of I_{γ_1}, in which $J_n = O(k^{-n})$.

In the light of this analysis we propose the following breakdown of the integral in (4):

$$I_{\gamma_1} = J(\tau) + I_{\gamma T} \;,$$

where

$$J(\tau) \approx J_1(\tau) \;, \tag{7}$$

and $I_{\gamma T}$ is the integral over a truncated interval $[\tau, X]$ with $\tau \leq X$ and $\tau < x_r$. Within these constraints τ is chosen to satisfy relative and absolute error criteria. We estimate the relative error in approximation (7) by the following upper bound on J_2/J_1:

$$E_r(\tau) = \left[\frac{g''(\tau)}{|g'(\tau)|} + \frac{3}{2}\left[\frac{1}{g_1(\tau)} + \frac{1}{g_2(\tau)}\right]\right]\frac{1}{k|g'(\tau)|} \tag{8}$$

Here $|f'(\tau)/f(\tau)|$ in J_2 has been replaced by an upper bound which is expected to hold always [7(p.598)]. We estimate the absolute error in approximation (7) by the following upper bound on J_2:

$$E_a(\tau) = E_r(\tau)\,\frac{|f(\tau)|}{k|g'(\tau)|} \tag{9}$$

Equations (8) and (9) usually give conservative estimates of the relative and absolute errors in approximation (7). We choose τ to be the minimum of τ_a, τ_r, and X, where τ_r satisfies

$$E_r(\tau_r) = 0{\cdot}2 \ , \qquad (10)$$

and τ_a satisfies

$$E_a(\tau_a) = \epsilon \ , \qquad (11)$$

where ϵ is chosen to give the required accuracy in I_{γ_1}. Both $E_r(x)$ and $E_a(x)$ are infinite at $x=x_r$ and tend to zero as $x\to-\infty$. A graphical examination suggests that $E_a(x)$ and $E_r(x)$ are monotonic in $(-\infty,x_r)$ for typical geometries and admittance values, so that τ_r and τ_a are uniquely defined.

The effect of the approximation (7) is to replace the problem of evaluating the integrand in (4) over the infinite interval $(-\infty,X]$, by the problem of evaluating the same integrand over the finite interval $[\tau,X]$. The approximation (7) removes the region over which the integrand is most oscillatory. The remaining integral over γ_T - that part of γ_1 near to the geometrical reflection point - can be evaluated efficiently by adaptive quadrature.

With this method it is necessary to ensure that the part of the integration path for which $J(\tau)$ is used, the interval $(-\infty,\tau]$, does not come within one wavelength of the source. So far this has only involved slight adjustments to τ when the source is low.

As the method stands, we have significantly reduced computation expense with no loss of accuracy. For a wide range of test cases run together on a Cyber 180-830, the total calculation time has been reduced by a factor of 9 over a previous method [1]. This has made it feasible to examine long distance propagation.

RESULTS

We can use φ given by the approximation (2) to examine propagation over flat ground through a homogeneous still atmosphere. The excess attenuation over spherical spreading due to the ground is given by

$$EA_1 = 20\log_{10}\left|\frac{e^{ikd}}{\varphi kd}\right|$$

To calculate the results presented here an absolute error limit of 0·001 in Q was specified. This gives an acceptable bound on ΔEA_1, the error in EA_1:

$$|\Delta EA_1| \leq 0{\cdot}013/10^{EA_1/20} \ ;$$

for example when EA_1=20dB, $|\Delta EA_1|\leq$0·13dB. To achieve this error limit in Q, the parameter ϵ in (11) was taken as

$$\epsilon = 0{\cdot}001\left|\frac{H_0^{(1)}(kD)}{4(\beta_1-\beta_2)}\right|$$

The known potentials G_{β_1} and G_{β_2} were calculated using an efficient and accurate algorithm [11,19].

Propagation from a source above rigid ground to a receiver above absorbing ground was examined. To this end β_1 was set to zero and $\beta_2(f)$ was calculated by the Delany and Bazley semi-empirical formula [12,13], with an effective flow resistivity of $10^5 kgs^{-1}m^{-3}$ chosen as a low value for grassland [14]. It was found that using two or three times this value caused only a small reduction in the magnitude of the results, and no change in the trends observed. The source and receiver heights were fixed at 1·5m.

For the present investigation a useful varable is

$$p_r = (X-d)/d \ .$$

When $0 \leq X \leq d$, p_r gives the proportion of rigid ground between the source and receiver.

Figures 1 show how EA_1 values for absorbing ground at four low frequencies are affected by the introduction of rigid ground from behind the source. Notice that when $p_r \leq 0$ or $p_r \geq 1$ the modelled ground behaves as an acoustically homogeneous plane. This indicates that the areas of flat ground behind the source and behind the receiver do not contribute noticeably to the ground effect attenuation at these long distances.

Looking only at the $p_r \leq 0$ cases in Figures 1(c) and (d): when d is greater than about 300 wavelengths we see an increase in EA_1 of approximately 6dB per doubling of d. This long distance effect at grazing incidence has been predicted in previous theoretical studies [15].

It is useful to note how EA_1 depends on p_r. Figure 1(a) illustrates that at very low frequencies there is a near linear decrease in EA_1 as the proportion of rigid ground between the source and reciever is increased. We see in Figure 1(b) that as the frequency rises a characteristic S-shaped curve develops. This characteristic curve is steepest when the admittance discontinuity in the ground approaches the source or reciever, suggesting that the type of ground close to the source or reciever is particularly important (c.f. the Dutch road traffic noise prediction model [16]). Figure 1(c) shows that this characteristic S-shaped curve is very well defined at 250Hz. In Figure 1(d) we see the beginnings of a pattern that intrudes into the S-shaped curve as the frequency rises. In this case, 500Hz, we see small oscillations in EA_1 at each end of the S-shaped curves. At higher frequencies (not shown) these oscillations extend considerably into each end of the S-shaped curve.

A further interesting feature to be observed in Figures 1(c) and (d) is the emergence of an approximately 3dB increase in EA_1 per doubling of d at a wide range of proportions of rigid ground ($0 \cdot 1 < p_r < 0 \cdot 9$). In common with the 6dB increase in EA_1 per doubling of d at $p_r = 0$, mentioned above, this 3dB per doubling of d occurs when d is greater than about 300 wavelengths.

At long distances attenuation due to air absorption of acoustic energy is significant. We can estimate a more practical quantity, the third-octave band excess attenuation due to air and ground, by

$$EA_3 = EA_1 + EA_2 .$$

where EA_2 is the predicted third-octave band free field air attenuation [17] at 20°C and 70% relative humidity. Here it has been assumed that EA_1 calculated at each third-octave band centre frequency is representative of the ground induced excess attenuation for the whole band.

Figure 2 shows EA_3 at the four long distances when $p_r=0\cdot5$. At frequencies less than 1kHz the ground effect attenuation dominates, causing a minimum at 315 Hz. At frequencies greater than 1kHz the air attenation dominates. These trends are to be observed whenever there is sufficient absorbing ground extending beneath the reciever: i.e. from about $p_r=0\cdot9$.

We can see further what the implications of these theoretical results are by applying them to a notional continuous broad-band environmental noise source. A simple spectral shape representative of a jet engine at full thrust has been used for this purpose. The approximate form of the spectrum used is

$$S_1 = \begin{cases} L \ \ dB \ , & f \leqslant 160 \text{ Hz} \ , \\ L - 8\log_{10}(f/160) \ dB \ , & f > 160 \text{ Hz} \ , \end{cases}$$

where S_1 is the third-octave band sound pressure level reduced to 1m in the free field, f is the third-octave band centre frequency, and L is determined by the operating parameters of the engine. The source is assumed to behave sufficiently like a point source at large distances for the theoretical results to be directly applicable. We define a total excess attenuation over spherical spreading for this source by

$$EA_4 = S_2 - (S_3 + 20\log_{10}d) \ \ dB(A) \ ,$$

where EA_4 is the broad band excess attenuation due to the ground effect and air absorption, S_2 is the total A-weighted sound pressure level of the notional source at 1m distance in the free field, and S_3 is the total A-weighted sound pressure level predicted at the reciever position.

While generating the EA_4 results, described below, the spectral composition of S_3 was noted. At d<1km S_3 is dominated by the frequency bands centred above 500Hz. It is only when d≥1km that S_3 is dominated by the less attenuated low frequency bands. For homogeneous absorbing ground this low frequency domination at long distances is interpreted in terms of the well known ground wave component of the acoustic potential field [15].

Figure 3 shows how EA_4 behaves. We can see that it is not possible to predict the EA_4 values at intermediate p_r from a linear interpolation between the values at $p_r=0$ and $p_r=1$. This is due to the growth, as f increases, of the curve shapes seen in figures 1. However, at the two longest distances we note that EA_4 at $p_r=0\cdot75$ is about 11dB(A) less than EA_4 at $p_r=0$. Also at these distances the EA_4 values in the range $0\leqslant p_r\leqslant 0\cdot75$ lie on straight lines. These features suggest that, at distances of one or two kilometres, the effect of a stretch of airport runway on the propagation from this type of broad-band noise source to a receiver located above grassland might be predicted by using

$$EA_4(p_r) = EA_4(0) - Cp_r, \quad 0 \leqslant p_r \leqslant 0\cdot8 \ , \qquad (12)$$

Figures 1. Dependence of excess attenuation due to the ground effect on the location of the admittance discontinuity.

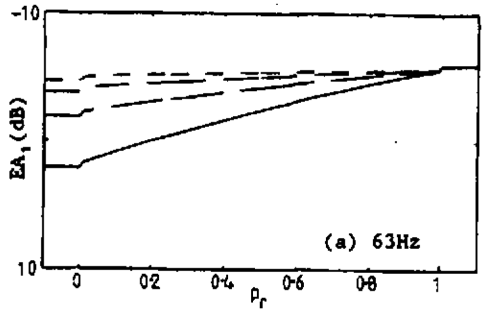

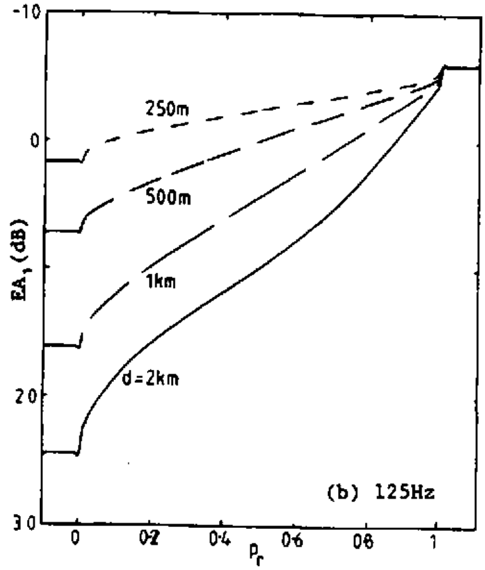

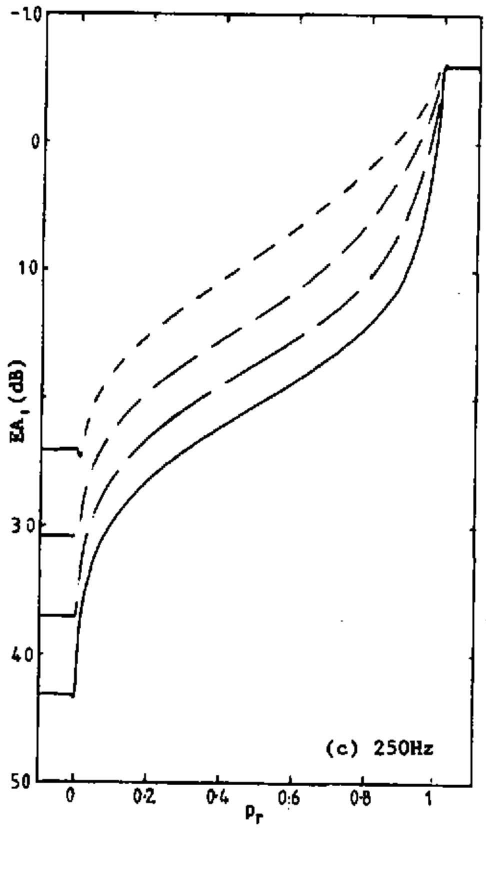

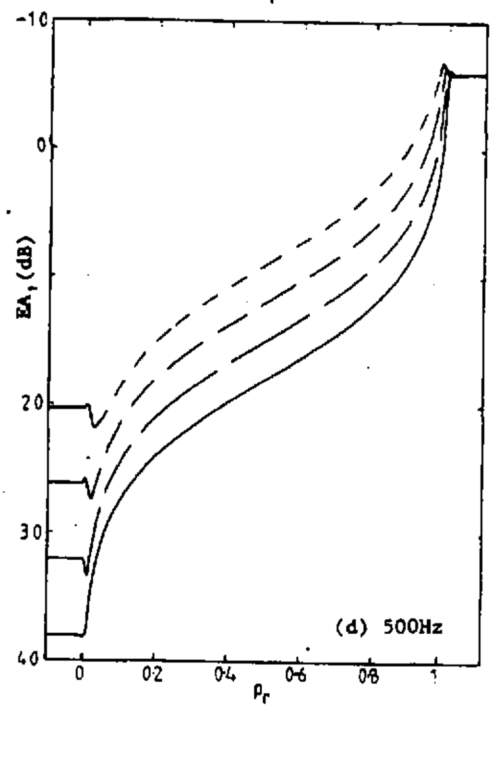

Figure 2. Estimated third-octave band excess attenuations due to ground effect and air absorption. p_r=0·5.

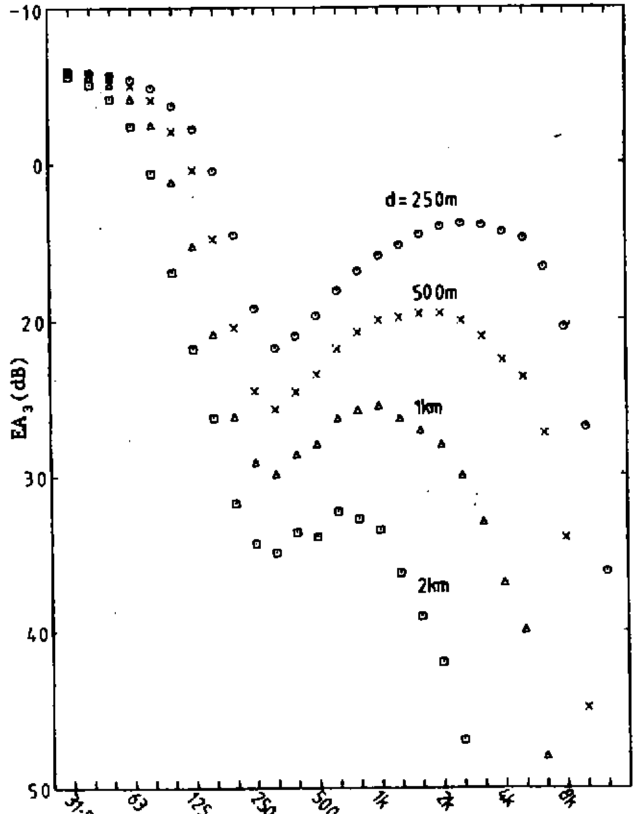

Figure 3. The effects of proportion of rigid ground on broad-band noise source excess attenuation over spherical spreading. Distances as for figure 2. Solid lines are equation (12).

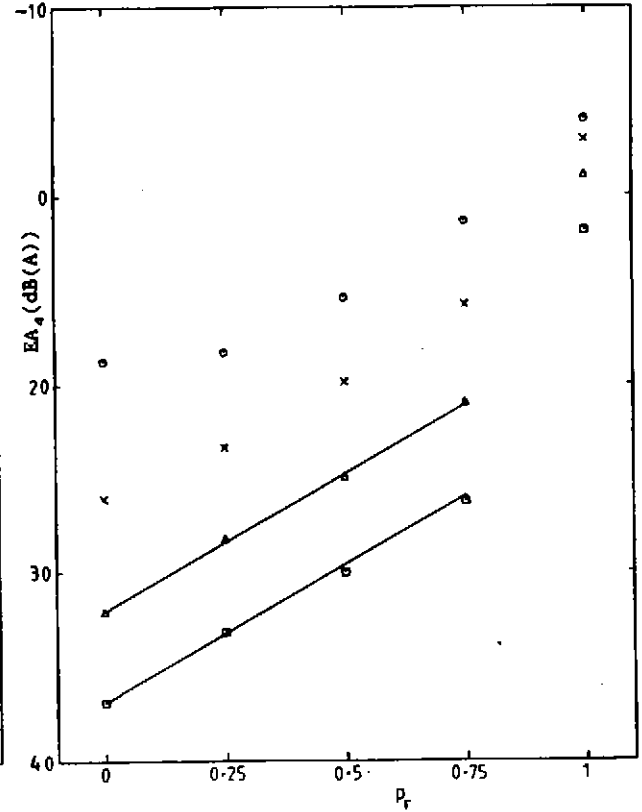

with C taking the value 14·7 for the results presented here.

A final interesting feature to note from figure 3 is the change in excess attenuation of the broad-band noise per doubling of distance at intermediate values of p_r. When $0{\cdot}25 \leq p_r \leq 0{\cdot}75$ we observe approximately a 5dB increase in EA_4 per doubling of d. No similarly simple trend is seen for propagation over the effectively homogeneous grounds. With the exception of the cases when p_r is greater than about 0·8, this result agrees reasonably with a commonly used 4dB extra attenuation (of perceived noise level) per doubling of d [18].

CONCLUSION

An improved calculation method has been presented for sound propagation over a straight line impedance discontinuity in flat ground. The method is derived from an asymptotic analysis at large wavenumber of an approximate form of the two dimensional boundary integral equation. Accuracy is adequate for the purpose of examining environmental noise propagation. A limitation of the method is the assumption of homogeneous still air and flat ground.

Results for grazing incidence monofrequency propagation show that the ground induced excess attenuation is most sensitive to the location of the impedance discontinuity when it is near the source or receiver. Only the ground between the source and receiver contributes noticeably to the excess attenuation. At large enough dimensionless source-receiver distances (kd), when the impedance discontinuity is in the central 4/5ths of the source-receiver range, propagation from above the rigid ground to above the absorbing ground shows a 3dB increase in excess attenuation per doubling of source-receiver distance.

Results for the excess attenuation, including air absorption, of a broad-band A-weighted notional environmental noise source show that the excess attenuation is most sensitive to the location of the impedance discontinuity when it is near the receiver. When the impedance discontinuity is in the central half of the source-receiver range, a 5dB(A) increase in excess attenuation per doubling of source-receiver distance is observed.

REFERENCES

[1] S.N.Chandler-Wilde, D.C.Hothersall. Sound propagation above an inhomogeneous impedance plane. J.Sound Vib.98, 475-91, 1985.

[2] M.Naghieh, S.I.Hayek. Diffraction of a point source by two impedance covered half-planes. J.Acoust.Soc.Am.69, 629-37, 1981.

[3] B.A.de Jong, A.Moerkerken, J.D.van der Toorn. Propagation of sound over grassland and over an earth barrier. J.Sound Vib.86, 23-46, 1983.

[4] J.Durnin, H.L.Bertoni. Acoustic propagation over ground having

inhomogeneous surface impedance. J.Acoust.Soc.Am.70, 852-9, 1981.

[5] K.B.Rasmussen. A note on the calculation of sound propagation over impedance jumps and screens. J.Sound Vib.84, 598-602, 1982.

[6] S.N.Chandler-Wilde, D.C.Hothersall. Developments in BIE methods for outdoor sound propagation. Acoustics '89, Oxford, April 1989.

[7] S.N.Chandler-Wilde. Ground effects in environmental sound propagation. Ph.D. thesis, Univ. Bradford, 1988.

[8] C.Klein, H.Myncke. Sound field above an impedance discontinuity. 3rd Fed.Acoust.Soc.Eur.Cong., 471-4, Gottingen, Sept.1982.

[9] C.M.Bender, S.A.Orszag. Advanced Mathematical Methods for Scientists and Engineers. McGraw-Hill, N.Y., 1978.

[10] D.Habault. Sound propagation above an inhomogeneous plane: boundary integral equation methods. J.Sound Vib.100, 55-67, 1985.

[11] S.N.Chandler-Wilde, D.C.Hothersall. Propagation from a line source above an impedance plane. Proc.Inst.Acoust.10, 523-31, 1988.

[12] M.E.Delany, E.N.Bazley. Acoustical properties of fibrous absorbent materials. App.Acoust.3, 105-16, 1970.

[13] C.I.Chessell. Propagation of noise along a finite impedance boundary. J.Acoust.Soc.Am.62, 825-34, 1977.

[14] T.F.W.Embleton, J.E.Piercey, G.A.Daigle. Effective flow resistivity of ground surfaces determined by acoustical measurements. J.Acoust.Soc.Am.74, 1239-44, 1983.

[15] K.Attenborough. Review of ground effects on outdoor sound propagation from continuous broadband sources. Appl.Acoust.24, 289-319, 1988.

[16] A.Moerkerken. The Netherlands Prediction Model for Outdoor Noise Propagation. Directoraat-Generaal voor de Milieuhygiene, Ministerie van Volkshuisvesting Ruimtelijke Ordening en Milieubeheer, Leidschendam, The Netherlands, 1986.

[17] British Standards Institution. Method for describing aircraft noise heard on the ground. British Standard 5727, H.M.S.O., 1979.

[18] L.I.C.Davies. A guide to the calculation of NNI. Direct.Operat.Res. Anal.Comm.7908, 2nd ed., C.A.A., London, 1981.

[19] S.N.Chandler-Wilde, D.C.Hothersall. On the Green function for two-dimensional acoustic propagation above a homogeneous impedance plane. Sub. for pub. to J.Acoust.Soc.Am.